A Sliding Mode Control Architecture for Autonomous Driving in Highway Scenarios Based on Quadratic Artificial Potential Fields

A Sliding Mode Control Architecture for Autonomous Driving in Highway Scenarios Based on Quadratic Artificial Potential Fields

Elisabetta Punta, *Senior Member, IEEE*, Massimo Canale, *Member, IEEE*, Francesco Cerrito, *Graduate Student Member, IEEE*, and Valentino Razza, *Member, IEEE*

***Abstract*—An approach for automated driving in highway scenarios based on Super-Twisting (STW) Sliding Mode Control (SMC) methodologies supported by the use of Artificial Potential Fields (APF) is presented. The use of APF allows us to propose an effective SMC solution based on the gradient tracking (GT) principle. In this regard, a novel formulation of the APF functions is introduced that exploits a sequence of attractive quadratic functions. This solution simplifies the computation of the fields and allows for trajectory generation with improved regularity properties. Extensive simulation tests, as well as comparisons with baseline and state of the art solutions, show the effectiveness of the proposed approach.**

***Index Terms*—Autonomous vehicles, automotive control, variable-structure/sliding-mode control.**

I. Introduction

IN RECENT decades, autonomous driving (AD) has gained interest as a way to achieve safer and more sustainable transportation systems. An AD system must integrate a path planner and path-tracking logic. The path planner builds a collision-free trajectory based on the measurements of the vehicle sensors. Traditional path-planning algorithms are graph-based or gradient-based techniques. Among the graph-based, the most common algorithms are Dijkstra (see, e.g., [1]) and A* (see, e.g., [2]). The main drawbacks of graph-based algorithms are the high complexity and computational costs. Studies to overcome such limitations can be found in, e.g., [3], [4]. However, the manageable search space is discrete, and the generated path may lead to high jerk values.

Received 16 September 2024; revised 15 November 2024; accepted 3 December 2024. Date of publication 16 December 2024; date of current version 26 December 2024. This work was supported in part by the Project Piano Nazionale di Ripresa e Resilienza (PNRR)-Next Generation Europe, which has funded by the European Union and the Italian Ministry of University and Research–DM 117/2023. Recommended by Senior Editor C. Manzie. *(Corresponding author: Massimo Canale.)*

Elisabetta Punta is with the Consiglio Nazionale delle Ricerche, CNR-IMATI, 27100 Pavia, Italy (e-mail: elisabetta.punta@cnr.it).

Massimo Canale and Francesco Cerrito are with the Department of Control and Computer Engineering, Politecnico di Torino, 10129 Turin, Italy (e-mail: massimo.canale@polito.it; francesco.cerrito@polito.it).

Valentino Razza are with the Department of Management and Production Engineering, Politecnico di Torino, 10129 Turin, Italy (e-mail: valentino.razza@polito.it).

Digital Object Identifier 10.1109/LCSYS.2024.3518927

However, gradient-based techniques can produce a collision-free trajectory with a small computation effort. They mostly rely on the APF algorithm, introduced in [5] for industrial and mobile robotics applications. In this approach, repulsive and attractive forces represent, respectively, obstacles and goals. Exploiting the gradient of the resulting field, the desired trajectory can be evaluated and updated to account for scenario changes (see, e.g., [6]). One of the main drawbacks of APF-based algorithms is the suboptimal solution. The APF goal is to make the gradient slope zero. Once this objective is reached, the algorithm cannot explore new search space and may get stuck in a local minimum [7]. Combining APF with other path-planning techniques can solve this problem (see [8]). APFs can easily be combined with control algorithms aiming to minimize a valued function or follow a descent gradient to design a path-tracking algorithm. While APF-based approaches have shown promise [9], their application to general road scenarios is complicated by the significant challenge of obtaining accurate, real-time mathematical formulations of APFs that can effectively model complex road geometries [10]. Furthermore, unlike robotics, automotive applications demand strict lane-center tracking and adherence to prescribed regulations.

The SMC [11] is a nonlinear control technique aiming to drive the system trajectory along a sliding surface, suitably defined to guarantee stability and desired performances. APFs are integrated into SMC by explicitly considering the field gradient in the sliding surface definition (see, e.g., [12]). Several applications of APF combined with SMC are proposed in different fields in the literature. In [13], [14], SMC and APF combinations are proposed for spacecraft maneuvers in the presence of obstacles.

In the automotive field, some remarkable results of SMC and APF are given. Longitudinal control is considered in [15], where the stabilization of a vehicle platoon is proposed through the time-headway dynamics controller. In [16], the authors propose an adaptive cruise control with collision avoidance. The lane-keeping and obstacle avoidance problem is considered in [9], where the APFs are generated through data from a single camera. The proposed solution defines APF as step slopes while approaching lane boundaries, creating a low potential safe area in the center of the lane. An adaptive APF is presented in [17], where the lane-keeping APFs are exponential or rapidly changing functions when the vehicle is

in the lane center or the proximity of the boundaries, respectively. SMC methodologies have been recently successfully employed in AD through STW algorithm. In particular, in [18], an interesting SMC-STW solution based on backstepping is introduced for path tracking. In the described SMC-STW approach, since the path is predefined, adaption to traffic conditions is prevented.

This letter proposes an APF-SMC combined strategy for a Level 3 autonomous vehicle in a highway scenario, according to driving automation levels from the Society of Automobile Engineers (see [19]). In such a context, emergency maneuvers are not considered. In particular, a novel APF formulation is proposed to manage the highway-relevant maneuvers, i.e., lane keeping and lane changing, where a target point ahead is defined at each sample time. The APFs are combined into a SMC-STW strategy, guaranteeing the control input continuity. The main features of the proposed solution are:

- we introduce a unique architecture for path planning and path tracking based on APFs, capable of handling all the driving functions involved in the highway scenario, i.e., lane keeping, overtaking and distance keeping from a previous slower vehicle;
- we propose a simplified APF formulation based on quadratic functions that rely on a single target point ahead, compared to standard approaches based on a combination of Gaussian functions. This reduces the computational burden and the sensor complexity;
- the desired lateral reference trajectory is derived from the APF gradient of such quadratic function, characterized by specific regularity properties that are functional for robustness analysis.

II. Problem Set-Up

In this letter, we deal with an automated vehicle, that is moving in a highway road in agreement with the SAE automation Level 3 features. Specifically, the vehicle executes a variety of standard highway maneuvers, including velocity tracking both in the presence and the absence of a heading vehicle, overtaking maneuvers, and precise lane keeping on straight and curved roads. We assume that the vehicle is provided by a full set of proprioceptive and exteroceptive sensors to detect all the relevant variables needed to implement the required automated driving maneuvers. To realize the automated driving functions discussed above, we introduce the control architecture reported in Fig. 1. Such an architecture, implements a SMC that exploits APF to obtain appropriate sliding surfaces for generating suitable trajectories to be tracked by the vehicle. In particular, in the scheme of Fig. 1, the on-board sensors of the vehicle provide the state of the vehicle in terms of the relevant longitudinal and lateral variables. Moreover, the radar and camera sensors acquire the environment information in terms of the surrounding vehicle position and speed and lane borders and center location. Based on such information, the *APF* block, builds and locate the APF functions needed to accomplish the lateral driving task and generates the yaw angle reference ψ_{ref}. A Finite State Machine (FSM) handles the implementation of the needed maneuver and generates the speed reference v_{ref}. The references ψ_{ref} and v_{ref} are used by the *Sliding Manifold* block to obtain the sliding

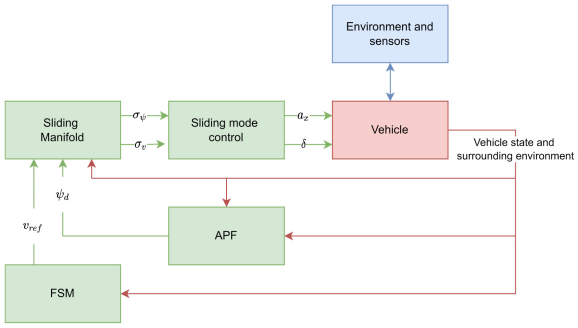

Fig. 1. The proposed control architecture.

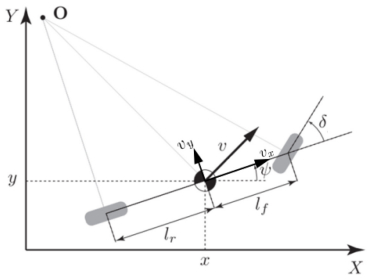

Fig. 2. Single-track Vehicle Model.

variables σ_ψ, σ_v employed by the *Sliding Mode Control* block to compute the control action in terms of steering angle δ and longitudinal acceleration a_x. The following sections, describe the technical details of each block.

III. Vehicle Model

The vehicle dynamics are described by the single-track model reported in Fig. 2 (see [20]). Given the absolute (X, Y) frame with the origin fixed at the initial vehicle position and orientation coinciding with the scenario environment coordinate x, y, and the yaw angle ψ specify the position and orientation of the vehicle center of gravity, v is the vehicle speed decomposed in its longitudinal and lateral components denoted as v_x and v_y, respectively, while δ is the steering angle. The longitudinal acceleration a_x and the steering angle δ are the inputs of the system.

Based on the just introduced model settings and accounting for the actuation dynamics characterized by the time constant τ, the longitudinal behavior of the vehicle is described by

$$\ddot{v}_x = \frac{1}{\tau}(-\dot{v}_x + a_x). \tag{1}$$

In this letter, we assume $\tau = 0.5$ s. The vehicle lateral dynamics are described by equations (2) and (3) that depend on the wheel cornering stiffnesses (C_f, C_r), the semi-wheelbases (l_f, l_r), the vehicle mass m, and the vehicle inertia along the vertical axis I_z

$$\dot{v}_y = -\frac{C_f + C_r}{m v_x} v_y + \frac{C_r l_r + C_f l_f}{m v_x}\dot{\psi} - v_x\dot{\psi} + \frac{C_f}{m}\delta, \tag{2}$$

$$\ddot{\psi} = \frac{C_f + C_r}{I_z v_x} v_y + \frac{C_r l_r^2 + C_f l_f^2}{I_z v_x}\dot{\psi} + \frac{C_f l_f}{I_z}\delta. \tag{3}$$

Nominal model (2)-(3) parameters, and relevant uncertainties, are reported in Table I.

TABLE I
VEHICLE PARAMETERS

Parameter	Value	Uncertainties
m	1575 kg	[0, 320] kg
I_z	3402 kg · m^2	[0 , 820] kg · m^2
l_f	1.2 m	[0, 0.152] m
l_r	1.8 m	[-0.152, 0] m
C_f	38000 N/rad	[-3800, 3800] N/rad
C_r	66000 N/rad	[-6600, 6600] N/rad

Remark 1: A point (X_o, Y_o) in the global inertial frame is the transform of a point (x_o, y_o) from the local frame as

$$\begin{bmatrix} X_o \\ Y_o \\ 1 \end{bmatrix} = \begin{bmatrix} \cos\psi & \sin\psi & x \\ -\sin\psi & \cos\psi & y \\ 0 & 0 & 1 \end{bmatrix} \begin{bmatrix} x_o \\ y_o \\ 1 \end{bmatrix}. \tag{4}$$

IV. APF FOR AD PATH PLANNING

In the literature, several possible formulations have been presented to describe an AD scenario on a highway via APF. Often the generated APFs are computationally complex. The most common approach involves building a total APF as a superposition of the road APF, represented by repulsive walls instead of the outer lane lines, and the APFs related to obstacles or other cars that act as repulsive points, [21].

In this letter it is proposed a novel approach to the definition of APFs for highway scenarios.

It is assumed that at each sampling step, data is acquired via sensors and the behavioral logic determines the action to be performed and builds the appropriate APF. Therefore, at each sampling step the APF changes and evolves due to the ever-changing surrounding environment. Given lane boundary points in an absolute (X, Y) reference frame, a target point (X_{target}, Y_{target}) is defined and computed at each step. This target point creates an attractive potential field, guiding the vehicle toward the desired path.

The attractive APF is defined as the quadratic function

$$U_a = \frac{1}{2}\left[\left(X_{target} - X\right)^2 + \left(Y_{target} - Y\right)^2\right] \tag{5}$$

where (X_{target}, Y_{target}) is updated at each step.

According to the maneuver to perform, the goal point (X_{target}, Y_{target}) will remain at the centre of the lane (Lane Keeping) or will move to an adjacent lane in a certain amount of time (Lane Changing).

The Lane Keeping (LK) feature entails keeping the vehicle at the centre of the lane along which the vehicle itself is travelling. The vehicle acquires data regarding the position of the lane boundaries in its own (X, Y) frame and can determine the position of the central point of the lanes as well. It is possible to define a target point (X_{target}, Y_{target}), which moves along the current lane as the vehicle moves forward. The point (X_{target}, Y_{target}) is defined as the center of the current lane at a fixed longitudinal distance from the vehicle. As the vehicle follows the desired longitudinal dynamics (i.e., travels along the lane), the target position (X_{target}, Y_{target}) changes. Even in the presence of a curve (necessarily with a radius of curvature $R > 500$m since it is on a highway) the target point (X_{target}, Y_{target}) will direct the vehicle to follow the correct trajectory.

The Lane Changing (LC) maneuver is performed whenever a vehicle needs to move into an adjacent lane to overtake and re-enter or move to the rightmost lane. The APF definition for LC follows the same premise as the LK one with one significant change. The target point (X_{target}, Y_{target}) not only moves along the direction of travel but also moves into the adjacent lane from the current lane based on the requested maneuver. When the vehicle needs to perform the LC maneuver, the behavioral logic needs to extract information not only about the current lane, but also about the target lane.

A. APF Gradient Tracking for Path Following

The concept of GT-SMC was first introduced in [12], where the key idea consisted of regarding the gradient lines as the desired trajectories. The gradient was interpreted as a desired velocity field and the controller oriented the vehicle velocity vector co-linear to the gradient.

The goal of the path tracking controller is to orient the vehicle's longitudinal axis co-linear to the gradient of the attractive APF (5) generated at each time step by the target point (X_{target}, Y_{target}).

The "attractive force" $\boldsymbol{f}_a$ generated by the APF (5) is

$$\boldsymbol{f}_a = \nabla U_a = \begin{bmatrix} U_{ax} \\ U_{ay} \end{bmatrix} = \begin{bmatrix} \left(X_{target} - X\right) \\ \left(Y_{target} - Y\right) \end{bmatrix} \tag{6}$$

where ∇U_a is the gradient of the attractive APF (5).

Finally, the desired vehicle orientation, i.e., the desired yaw angle ψ_d, is evaluated as a function of the gradient

$$\psi_d = \arctan\left(\frac{U_{ay}}{U_{ax}}\right). \tag{7}$$

B. Behavioral Logic

A finite state machine (FSM) chooses the driving task based on the detected surrounding environment. In the highway scenario, the possible tasks are left or right lane change, lane keeping, target velocity tracking, and adapting cruise control (ACC). The outputs of the FSM are the target position (X_{target}, Y_{target}), used in the APF definition, and the target velocity for the longitudinal controller.

First, the current lane index $\ell = 1, 2, \ldots, n_\ell$ is evaluated, where 1 is the rightmost lane and n_ℓ is the number of available lanes, the FSM checks the presence of a slower vehicle ahead on the same lane. If a slower vehicle is present and $\ell < n_\ell$, then the FSM evaluates if the left LC maneuver is suitable, i.e., if moving to $\ell_{tar} = \ell + 1$. Otherwise, if $\ell > 1$, a right LC maneuver is considered, i.e., if moving to $\ell_{tar} = \ell - 1$. The LC maneuver can be performed if the target distance $d_{tar} = d_0 + t_H v_x$ is kept from any vehicle on the target lane ℓ_{tar}, where d_0 is the safety distance and t_H is the headway time. If no LC maneuver is planned, the FSM activates the LK.

Given the sensor data for each sample time t_0, we evaluate the current lane center (x_O, y_O) in the vehicle local frame at a fixed distance ahead, i.e., $x_O = K$, where K is the lookahead distance. For LK maneuvers, the target (X_{target}, Y_{target}) point is computed from (x_O, y_O) through (4). On the other hand, the LC begins at t_{ini}. We freeze the current value ℓ to design a smooth trajectory connecting the lane centers from ℓ to ℓ_{tar}

in a fixed maneuver time t_{LC}. Thus, for each sampling time $t_{ini} \leq t \leq t_{ini} + t_{LC}$, the FSM computes

$$d_{lane} = \ell_W + \frac{\alpha}{2}\left[1 - \cos\left(\pi \frac{t - t_{ini}}{t_{LC}}\right)\right] \tag{8}$$

where $\alpha = 1$ or $\alpha = -1$ if moving to the lane at the left or the right, respectively and ℓ_W is the lane width. Then, given the current value (x_O, y_O) for lane ℓ, the target position is computed applying (4) to $(x_O, y_O + d_{lane})$.

Remark 2: It is worth noting that this letter objective is the design of a Level 3 autonomous vehicle, where emergency maneuvers are demanded of the driver. The LC is performed if the safety distances are guaranteed at the new lane ℓ_{tar}. If the scenario undergoes significant changes within the next t_{LC} seconds, resulting in an emergency situation, it falls outside the scope of this letter.

Together with the APF target position, the reference velocity v_{ref} is computed given the current lane ℓ. The FSM considers three factors to compute v_{ref}: the user-selected velocity v_{max}, the comfort in terms of maximum lateral acceleration $a_{y,max}$, and the ACC maneuver. To preserve the passengers comfort, given the road curvature ρ from the on-board sensors, we get

$$v_{curve} = \sqrt{\rho\ a_{y,max}}. \tag{9}$$

Finally, the ACC mode is activated if a slower vehicle is ahead and the LK maneuver is performed. A smooth velocity trajectory is designed to move from the current speed v_{in} to the preceding vehicle speed v_{end}. To care about comfort performance, we consider a maximum absolute jerk and maximum absolute longitudinal acceleration values as j_{max} and $a_{x,max}$, respectively. A bang-bang trajectory $v_{link}(t)$ is evaluated for $t_{ini} \leq t \leq t_{ACC}$, where the jerk value $-j_{max}$ is kept till reaching the acceleration value $-a_{x,max}$. Then, the acceleration is kept constant before applying the maximum j_{max} to reach 0 acceleration and v_{end} velocity. The value t_{ACC} is defined as the v_{link} trajectory duration.

Then, the ACC reference velocity is given by

$$v_{ACC} = \begin{cases} v_{link}(t) & t_{ini} \leq t \leq t_{ACC}, \\ \frac{d - d_{tar}}{t_H} & t > t_{ACC}, \end{cases} \tag{10}$$

where d is the distance from the preceding vehicle, and the reference speed is given by

$$v_{ref} = \min\{v_{max}, v_{curve}, v_{ACC}\}. \tag{11}$$

V. Sliding Mode Control Strategy for AD

The proposed controller for the autonomous driving system consists of a longitudinal controller that regulates the vehicle speed and a lateral controller that steers the vehicle to follow the path, both of which are designed based on a second-order SMC, specifically the Super-Twisting SMC (STW-SMC) strategy, [11], [22].

A. APF Gradient Tracking STW-SMC: Sliding Output σ_ψ

The APF Gradient Tracking STW-SMC objective is to steer asymptotically to zero the yaw angle tracking error. It is chosen the sliding variable $\sigma_\psi = \dot{e}_\psi + \lambda_\psi e_\psi$, where $e_\psi = \psi - \psi_d$, ψ_d is computed according to (7), and $\lambda_\psi > 0$ is a positive constant parameter of the controller.

When a sliding motion is established on the sliding surface

$$\sigma_\psi = \dot{e}_\psi + \lambda_\psi e_\psi = 0, \tag{12}$$

system (3) behaves as a stable first order linear system in which the positive λ_ψ determines how quickly the yaw angle tracking error converges asymptotically to zero.

B. Longitudinal Speed STW-SMC: Sliding Output σ_v

The goal of the longitudinal speed tracking controller is to make the vehicle velocity profile asymptotically follow a reference profile $v_{ref}(t)$ given by (11) and determined by the type of maneuver the vehicle has to perform.

The sliding variable is defined as $\sigma_v = \dot{e}_v + \lambda_v e_v$, where $e_v = v_x - v_{ref}$ and $\lambda_v > 0$ is a positive constant parameter of the controller. On the corresponding sliding surface

$$\sigma_v = \dot{e}_v + \lambda_v e_v = 0, \tag{13}$$

the longitudinal velocity of the vehicle v_x tracks asymptotically the desired reference profile v_{ref}.

C. Lateral and Longitudinal Dynamics STW-SMC

Consider (1)-(3), (12) and (13), the time derivatives of the sliding outputs σ_ψ and σ_v are

$$\dot{\sigma}_i = h_i(t) + k_i u_i, \quad i = \psi,\ v, \tag{14}$$

where $h_\psi = \frac{C_f + C_r}{I_z v_x}(\dot{v}_y + \dot{\psi}) - (\ddot{\psi}_d + \lambda_\psi \dot{\psi}_d)$, $k_\psi = \frac{C_f l_f}{I_z}$, $u_\psi = \delta$ and $h_v = (\lambda_v - \frac{1}{\tau})\dot{v}_x - (\ddot{v}_{ref} + \lambda_v \dot{v}_{ref})$, $k_v = \frac{1}{\tau}$, $u_v = a_x$. Constant bounds $K_{im}, K_{iM} > 0$ for the gains k_i, $i = \psi, v$, are known such that $0 < K_{im} \leq k_i \leq K_{iM}$, $i = \psi, v$, Table II.

Remark 3: Consider the highway scenario without emergency maneuver, $v_x > 0$ (Level 3 AV application). $\dot{v}_y$ and $\ddot{\psi}$ are computed from (2) and (3), that are Lipschitz continuous functions. The chosen formulation for the APF (5) is an analytical polynomial function whose derivatives exist for any arbitrary order for a fixed value of (X_{target}, Y_{target}). Thus, ψ_d from (7) is bounded and differentiable for any derivative order almost everywhere. $\ddot{v}_x$ is Lipschitz continuous from (1). From (11), the reference v_{ref} is the minimum among continuous and bounded functions up to the third derivative order. In particular, v_{curve} is continuously differentiable thanks to restrictions from road construction normative regulations imposing continuity in the curvature ρ variations. Then v_{ref} is bounded for all its derivatives up to the third order almost everywhere, with the exceptions of the switching instants, i.e., when the min function sets a different reference curve for v_{ref} in (11).

Proposition 1: In the defined driving scenario, constants L_i, $i = \psi, v$ exist and are available to the controllers such that

$$L_i \geq 0 \colon |\dot{h}_i| \leq L_i,\ i = \psi, v, \tag{15}$$

$\dot{h}_\psi = \frac{C_f + C_r}{I_z v_x}(\dot{v}_y - \frac{\dot{v}_x}{v_x} v_y) + \frac{C_r l_r^2 + C_r l_f^2}{I_z v_x}(\ddot{\psi} - \frac{\dot{v}_x}{v_x}\dot{\psi}) - (\psi_d^{(3)} + \lambda_\psi \ddot{\psi}_d)$ and $\dot{h}_v = (\lambda_v - \frac{1}{\tau})\ddot{v}_x - (v_{ref}^{(3)} + \lambda_v \ddot{v}_{ref})$.

Proof: The driving scenario according to Remark 3 implicitly defines a nonempty compact set $\mathcal{D}$. In such a set $\mathcal{D}$, the functions $\dot{h}_i : \mathcal{D} \to IR$, $i = \psi, v$, are continuous, then, thanks to the Weierstrass Theorem, $\dot{h}_i$, $i = \psi, v$, are bounded. ■

TABLE II
CONTROLLERS PARAMETERS

Parameter	Value	Parameter	Value
λ_ψ	30	λ_v	1
L_ψ	$2.9 \cdot 10^{-5}$	L_v	0.5
c_ψ	$8.2 \cdot 10^{-3}$	c_v	1.06
b_ψ	$3.3 \cdot 10^{-5}$	b_v	0.55

TABLE III
MAXIMUM LATERAL ERROR FORM LANE CENTER

Controller	Without uncertainties	With uncertainties
STW-SMC	3.75 cm	4.85 cm
SMC	9.65 cm	12.70 cm
PI	48.33 cm	58.30 cm

Table II reports the found values of L_i, $i = \psi, v$. The control laws u_i, $i = \psi, v$, are designed by the STW-SMC algorithm

$$u_i = -c_i \, |\sigma_i|^{\frac{1}{2}} \operatorname{sign}(\sigma_i) + w_i, \qquad \dot{w}_i = -b_i \operatorname{sign}(\sigma_i), \quad i = \psi, v, \tag{16}$$

where σ_i, $i = \psi, v$, are the sliding variables in (12) and (13), $c_i K_{im} > 1.5 L_i^{\frac{1}{2}}$ and $b_i K_{im} > 1.1 L_i$, $i = \psi, v$, are the parameters of the two controllers. The continuous control laws designed by the STW-SMC algorithm (16) and applied to (1)-(3) guarantee the convergence of both σ_i and $\dot{\sigma}_i$, $i = \psi, v$, to zero in finite time, [11], [22].

D. STW Filtering of the Longitudinal Speed Reference

An STW filtering, [23], of the longitudinal speed reference $v_{ref}(t)$ given by (11) is introduced to prevent sudden changes and variations in the vehicle acceleration, thus improving the smoothness of the computed control action a_x as well as the safety and comfort performance for passengers.

The STW filter is defined by the auxiliary system $\dot{z} = \eta$ and $s = z - v_{ref}(t)$, implementing the STW continuous law $\eta = -c_F |s|^{1/2} \operatorname{sign}(s) + w_F$, with $\dot{w}_F = -b_F \operatorname{sign}(s)$, that steers both s and $\dot{s}$ to 0 in finite time. Use η as the equivalent $\dot{v}_{ref_{eq}}$ in (13), [23]. Notice that the STW filter on the longitudinal speed reference described here improves the regularity properties of the desired trajectory.

VI. NUMERICAL SIMULATIONS

The vehicle performance is evaluated employing (1)-(3) implemented in a Simulink model. To evaluate the effectiveness of the proposed solution, extensive simulations were conducted under both nominal conditions and in the presence of model parameters uncertainties. All the parameters are detailed in Table I. The variations in the parameters account for different conditions, such as the presence of additional passengers and the deterioration of tire conditions. Furthermore, the proposed approach is compared against a baseline PI yaw-rate-based solution having a similar architecture presented in [24] and a state-of-art sliding mode controllers detailed in [25] and [18].

A 2.8 km two-lane highway road scenario has been designed to comprehensively replicate potential driving scenarios under typical conditions. The path is made of a one-way roadway with two 3.6 m wide lanes. The geometric layout of the simulated environment, depicted in Fig. 3, is designed as follows. A straight 823 m path, followed by two 30° turns, left then right, of 750 m minimum radius. Then, a 823 m

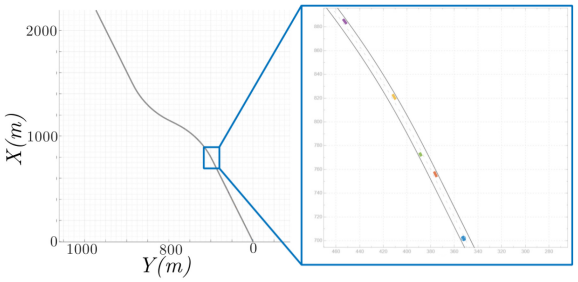

Fig. 3. Double-bend scenario.

straight path ends the scenario. The road path and independent vehicles representing the road traffic are simulated through the Matworks Driving Scenario Toolbox.

The simulation is divided into three sequential sections to evaluate the considered maneuvers. In the initial phase, the ego-vehicle traversed the first straight road, accelerating from an initial speed of approximately 118 km/h to the reference speed of 130 km/h. Upon approaching the double-curve section, the ego vehicle encounters three slower vehicles ahead, moving at 80 km/h. The second lane has no approaching vehicles, and the ego can begin the overtaking maneuver by moving to the left lane. Ahead on the second lane, the ego vehicle finds a car traveling at 110 km/h, already performing the overtaking maneuver. Thus, the ego vehicle must activate the adaptive cruise control system till the car ahead ends the overtaking. As the leading vehicle returns to the rightmost lane, the ego-vehicle completes the overtaking maneuver and, subsequently, rejoins the rightmost lane.

During the initial phase of the simulation ($t \in (0\,\text{s}, 18\,\text{s})$), the vehicle accelerated uniformly to reach the target speed of 130 km/h while keeping a constant yaw angle on a straight path. At $t = 18$ s, the behavioral logic transitioned to state 1 (moving left), initiating the overtaking maneuver. The controller acts on the vehicle's steering angle to execute the maneuver successfully. Additionally, the ego-vehicle dynamically adjusted its speed based on both the road curvature and the speed of the slower leading vehicle. As illustrated in Fig. 4C, adaptive cruise control maneuver was completed at $t = 29$ s, maintaining a consistent safety distance of 57 meters.

At $t = 58$ s, the vehicle returned to the straight road, maintaining a reference speed of 130 km/h. The vehicle successfully completed the overtaking maneuver at $t = 73$ s when the safety conditions for rejoining the rightmost lane were met.

As shown in Fig. 4, the filter applied to the reference speed effectively reduces the acceleration control action effort and rate. Consequently, the reduction in jerk enhances passenger comfort. Furthermore, Fig. 5A, B, and C illustrate that the strip related to the applied disturbances is very narrow, indicating robust control performance against model uncertainties. As shown in Fig. 5A, the applied model uncertainties particularly affect the steering angle control input. Nevertheless, due to the controller's action, both the vehicle's yaw angle (Fig. 5B) and its distance from the center lane (Fig. 5C) are minimally impacted. Finally, Fig. 5D illustrates the vehicle's movement to the left lane and its subsequent return to the right lane. In comparison to state-of-the-art approaches [24] and [25], the proposed approach demonstrates superior performance by

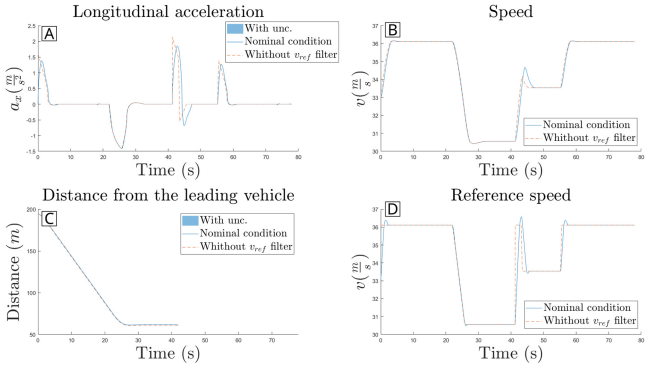

Fig. 4. Simulation results - Longitudinal dynamics.

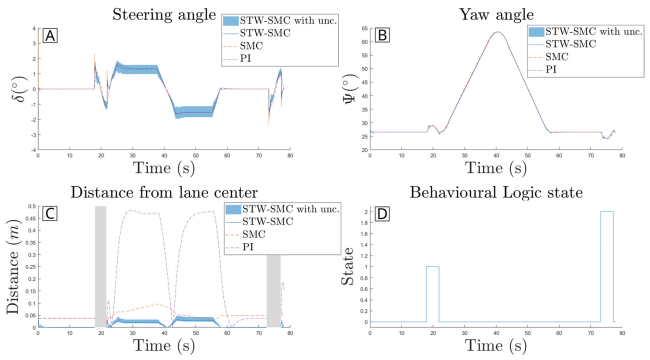

Fig. 5. Simulation results - Lateral dynamics.

reducing lateral error in both ideal and perturbed scenarios III. Additionally, it augments control action performance by decreasing both the effort and rate of the control inputs, thereby enhancing passenger comfort (Fig. 5A).

VII. Conclusion

This letter presents an automated driving approach in highway scenarios based on SMC methodologies, supported by quadratic APFs. In this regard, a new formulation of the APF functions has been introduced that exploits a sequence of attractive quadratic functions centered on the target points of the planned trajectory. In this way the gradient computation is more effective, leading to more accurate trajectory tracking and convergence results. Using the STW algorithm to filter the speed reference has improved the smoothness properties of the computed control action, increasing the comfort performance. Extensive simulation tests including a sensitivity analysis, together with comparisons with baseline and state of the art solutions showed the effectiveness and robustness properties of the proposed approach.

References

[1] D. Delling, A. V. Goldberg, A. Nowatzyk, and R. F. Werneck, "PHAST: Hardware-accelerated shortest path trees," *J. Parallel Distrib. Comput.*, vol. 73, no. 7, pp. 940–952, 2013.

[2] X. Tang, T. Zhou, J. Yu, J. Wang, and Y. Su, "An improved fusion algorithm of path planning for automated guided vehicle in storage system," in *Proc. IEEE 4th Int. Conf. Comput. Commun. (ICCC)*, 2018, pp. 510–514.

[3] L. Yeong-Ho, K. Yeong-Jun, J. Da-Un, and W. Ihn-Sik, "Development of an integrated path planning algorithm for autonomous driving of unmanned surface vessel," in *Proc. 20th Int. Conf. Control, Autom. Syst. (ICCAS)*, 2020, pp. 27–32.

[4] X. Zhong, J. Tian, H. Hu, and X. Peng, "Hybrid path planning based on safe a* algorithm and adaptive window approach for mobile robot in large-scale dynamic environment," *J. Intell. Robot. Syst.*, vol. 99, no. 1, pp. 65–77, 2020.

[5] O. Khatib, "Real-time obstacle avoidance for manipulators and mobile robots," in *Proc. IEEE Int. Conf. Robot. Autom.*, 1985, pp. 500–505.

[6] P. B. Kumar, H. Rawat, and D. R. Parhi, "Path planning of humanoids based on artificial potential field method in unknown environments," *Expert Syst.*, vol. 36, no. 2, 2019, Art. no. e12360.

[7] F. Bounini, D. Gingras, H. Pollart, and D. Gruyer, "Modified artificial potential field method for online path planning applications," in *Proc. IEEE Intell. Veh. Symp. (IV)*, 2017, pp. 180–185.

[8] M. Reda, A. Onsy, A. Y. Haikal, and A. Ghanbari, "Path planning algorithms in the autonomous driving system: A comprehensive review," *Robot. Auton. Syst.*, vol. 174, Apr. 2024, Art. no. 104630.

[9] L. Capito, U. Ozguner, and K. Redmill, "Optical flow based visual potential field for autonomous driving," in *Proc. IEEE Intell. Veh. Symp. (IV)*, 2020, pp. 885–891.

[10] P. Lin, E. Javanmardi, J. Nakazato, and M. Tsukada, "Potential field-based path planning with interactive speed optimization for autonomous vehicles," in *Proc. 49th Annu. Conf. IEEE Ind. Electron. Soc. (IECON)*, 2023, pp. 1–6.

[11] Y. Shtessel, C. Edwards, L. Fridman, and A. Levant, *Sliding Mode Control and Observation*. New York, NY, USA: Springer, 2014.

[12] J. Guldner and V. I. Utkin, "Sliding mode control for gradient tracking and robot navigation using artificial potential fields," *IEEE Trans. Robot. Autom.*, vol. 11, no. 2, pp. 247–254, Apr. 1995.

[13] M. Mancini, N. Bloise, E. Capello, and E. Punta, "Sliding mode control techniques and artificial potential field for dynamic collision avoidance in rendezvous maneuvers," *IEEE Control Syst. Lett.*, vol. 4, pp. 313–318, 2020.

[14] L. Cao, D. Qiao, and J. Xu, "Suboptimal artificial potential function sliding mode control for spacecraft rendezvous with obstacle avoidance," *Acta Astronautica*, vol. 143, pp. 133–146, Feb. 2018.

[15] K. B. Devika, G. Rohith, and S. C. Subramanian, "Potential function-based string stable controller for heavy road vehicle platoons," *IEEE Access*, vol. 9, pp. 156274–156282, 2021.

[16] B. Ganji, A. Z. Kouzani, S. Y. Khoo, and M. Shams-Zahraei, "Adaptive cruise control of a HEV using sliding mode control," *Expert Syst. Appl.*, vol. 41, no. 2, pp. 607–615, 2014.

[17] Y. Zhang, K. Liu, F. Gao, and F. Zhao, "Research on path planning and path tracking control of autonomous vehicles based on improved APF and SMC," *Sensors*, vol. 23, no. 18, p. 7918, 2023.

[18] D. Ao, W. Huang, P. K. Wong, and J. Li, "Robust backstepping super-twisting sliding mode control for autonomous vehicle path following," *IEEE Access*, vol. 9, pp. 123165–123177, 2021.

[19] *Taxonomy and Definitions for Terms Related to Driving Automation Systems for On-Road Motor Vehicles*, SAE Standard J3016_202104, 2021.

[20] R. Rajamani, *Vehicle Dynamics and Control* (Mechanical Engineering Series). New York, NY, USA: Springer, 2011.

[21] M. Canale and V. Razza, "Automated driving control in highway scenarios through a two-level hierarchical architecture," *IEEE Access*, vol. 12, pp. 86470–86486, 2024.

[22] A. Levant, "Universal single-input-single-output (SISO) sliding-mode controllers with finite-time convergence," *IEEE Trans. Autom. Control*, vol. 46, no. 9, pp. 1447–1451, Sep. 2001.

[23] E. Punta, "First and second order sliding mode equivalent signals and practical approximability in the implementation," in *Proc. 16th Int. Workshop Var. Struct. Syst. (VSS)*, 2022, pp. 1–5.

[24] A. Bonci, A. Di Biase, M. C. Giannini, and S. Longhi, "Yaw rate-based PID control for lateral dynamics of autonomous vehicles, design and implementation," in *Proc. IEEE 28th Int. Conf. Emerg. Technol. Factory Autom. (ETFA)*, 2023, pp. 1–8.

[25] G. Tagne, R. Talj, and A. Charara, "Design and comparison of robust nonlinear controllers for the lateral dynamics of intelligent vehicles," *IEEE Trans. Intell. Transp. Syst.*, vol. 17, no. 3, pp. 796–809, Mar. 2016.

Open Access funding provided by 'Politecnico di Torino' within the CRUI CARE Agreement